THE UNIVERSITY OF MANITOBA

THE DEFORMATION BEHAVIOR OF PRECIPITATION HARDENED Co - Ni - Cr - Ti SUPERALLOYS

by

D. W. CHUNG

A THESIS

SUBMITTED TO THE FACULTY OF GRADUATE STUDIES

IN PARTIAL FULFILMENT OF THE REQUIREMENTS FOR THE DEGREE

OF DOCTOR OF PHILOSOPHY

DEPARTMENT OF MECHANICAL ENGINEERING

METALLURGY

WINNIPEG, MANITOBA

February, 1976

"THE DEFORMATION BEHAVIOR OF PRECIPITATION HARDENED
Co - Ni - Cr - Ti SUPERALLOYS"

by
D. W. CHUNG

A dissertation submitted to the Faculty of Graduate Studies of the University of Manitoba in partial fulfillment of the requirements of the degree of

DOCTOR OF PHILOSOPHY

ABSTRACT

The Deformation Behavior of Co - Ni - Cr - Ti Alloys

by

D. W. Chung

The deformation behavior of three Co - Ni - Cr base precipitation hardenable alloys with different Ti contents has been studied. On ageing at 700, 800 and 900° C the main precipitating phase was found to be the γ' phase, with an ordered F.C.C. structure, in a F.C.C. matrix. The γ' phase precipitated coherently along <100> matrix directions in cuboid shape and the precipitate-lattice mismatch was 1.3%. The coarsening kinetics of γ' precipitate in all the three alloys followed the time-law predictions of the Lifshitz-Wagner theory of diffusion controlled growth at all the ageing temperatures. The particle size distribution of γ' was significantly broader than the distribution predicted by the Lifshitz-Wagner theory. This appears to be in agreement with previous studies on other alloy systems and may be attributable to the relatively large lattice mismatch between the precipitate and the matrix. The effect of volume fraction of γ' on its coarsening rate was negligible and thus the present system did not follow the "Modified Lifshitz-Wagner theory", which takes into consideration the volume fraction of the growing phase.

The strengthening mechamisms in terms of dislocation-particle interaction, have also been studied. It was observed that when the γ' particle size is smaller than 28 $\mathring{A}$ they are sheared by

the glide dislocations, which move in pairs, and when it is larger than 56 Å they are passed by the single glide dislocations leaving loops around the precipitate particles. Both types of interactions were observed when the particle size was between 28 - 56 Å. During the early stages of ageing, when the particles are sheared by pairs of dislocations, the tensile test results seem to fit both the coherence hardening model of Gerold and Haberkorn and the order hardening model of Brown and Ham. However, the nature of the $\Delta\tau$ - $r_s^{1/2}$ curves and the determination of antiphase boundary energy from them seemed to favour the order hardening mechanism. During the Orowan hardening the suggestion of Hirsch and Humphreys that both edge and screw dislocations require the same stress to by-pass the particles, seems to be correct.

Serrated yielding was also observed in the temperature range of 300 $\sim$ 600° C. The onset of serrated yielding is shown to be in agreement with the static strain ageing model. The critical strain to serrations decreases with increasing solute concentration in the solid-solution and with ageing time in aged conditions. This behavior can be explained in terms of a change in obstacles spacing if solute atoms are the major obstacles to dislocation motion in the solid solution condition and if γ' particles are the obstacles in the aged condition. The results also indicate a consistancy with Saada's model for vacancy production and a negligible change in the mobile dislocation density with strain.

The flow stresses in the temperature range of 23 to 900° C at various strain rates was also determined. In the temperature range

where serrated yielding was observed the 0.2% offset yield stress showed a characteristic temperature independence and also an inverse strain rate effect.

SYMBOLS

C	An average concentration in a system with a different particle size.
C_r	The equilibrium solutility of a one component particle with a radius r.
C_e	The equilibrium solubility of a particle of infinite radius in the external phase.
γ_s	The interfacial free energy of the particle-matrix interface.
Ω	Molar volume of a particle.
t	Ageing time of a system.
D	Diffusion coefficient of solute atoms in the matrix phase.
R	Gas constant; 1.987 cal/mole° K.
T	Absolute temperature.
r	The particle radius.
r^*	The critical particle radius; $\Sigma r_i / \Sigma r_i^2 = 1/r^*$ where i = 0, 1, 2, 3, ...
$\bar{r}$	The mean particle radius.
$\bar{r}_{(o)}$	The mean particle radius at t = 0.
$\bar{r}_{(t)}$	The mean particle radius at time t.
f_v	Volume fraction of particles.
$f(r,t)$	The distribution function of particle size, r, at time t.
Q	Activation energy for the coarsening process.
Z	The total number of particles per unit volume.
$g'(r,t)$; $f(r,t)/z$	
ρ	The dimensionless measure of particle size; $r/r^*_{(t)}$.

K A rate constant of the coarsening process for the spherical particle.

K' A rate constant of the coarsening process for the cuboid particles.

$g(t)$, $h(\rho)$ Help functions defined for growth kinetics in section (1.2).

ρ_M The maximum reduced particle size in dimensionless unit.

$\Gamma(f_v)$ A function of f_v; $\int_{8f_v}^{\infty} x^{-2/3} e^{-x} dx$.

$\bar{a}(t)$ The mean edge length of the cubic particles at time t.

$\bar{a}(o)$ The mean edge length of the cubic particle at time 0. $t = 0$.

F The force on an obstacle due to a dislocation and vice versa.

T^* The Dewit-Koehler approximation for the line tension.

τ Applied shear stress resolved in the slip direction in the slip plane.

ϕ Included angle between the arms of a dislocation at an obstacle.

b Burgers vector of a dislocation.

N_A The number of particle per unit area.

L Spacing between two obstacles.

L_o The mean planar spacing of obstacles; Orowan spacing.

L_s The square lattice spacing; $N_A^{-1/2}$.

L_1 The effective particle spacing at the first dislocation of a pair.

L'' The average distance between the force centers.

L_f The Friedel spacing.

τ_f The Friedel stress.

N_V The number of particles per unit volume

τ_o	The Orowan stress.
τ_1	The shear stress required to cut the particle by the first dislocation.
γ_{APB}	Anti-phase boundary energy.
r_s	The average radius of particle intersected by a slip band; $(\frac{2}{3})^{1/2} r$.
$\Delta\tau$	The increment of flow stress.
K_r	The maximum repelling force of the strain field of a single particle on a moving dislocation.
θ	The angle between the Burgers vector and the normal to the tangent of a curved segment of dislocation; $1/2\ (\pi - \phi)$.
ε	The "constrained" strain; coherency strain.
τ_m	The shear yield stress of the matrix phase.
τ_{edge}	The shear stress for edge dislocation
τ_{screw}	The shear stress for screw dislocation
G	Shear modulus.
X	Dipole width of a dislocation.
r_o	Inner cut off radius.
ν	Poisson ratio.
σ, σ_{edge}, σ_{screw}, σ_m	The macroscopic flow stress; for two phases edge dislocation, screw dislocation, and the matrix phase.
T_c	The ordering temperature.
S	The Bragg-Williams long range order parameter.
τ_p	The extra-hardening stress due to particle.
V_s	The velocity of the solute atoms.

ℓ	The effective radius of the solute atmosphere.
U_m	The solute-dislocation binding energy.
ε	Strain.
$\dot{\varepsilon}$	Strain rate.
V_D	The velocity of a dislocation around solute atmosphere.
Φ	An orientation factor upon which $\dot{\varepsilon}$ depends.
ρ_m	Mobile dislocation density.
ρ_T	Total dislocation density.
C_V	Vacancy concentration of alloy.
Q_m	Vacancy migration energy.
D_o	Pre-exponential diffusion coefficient.
ε_c	Critical strain for the onset of serrated yielding.
t_w	Waiting time of a dislocation at obstacles.
t_a	Ageing time of a dislocation.
t_f	Dislocation flight time.
$\bar{V}_j$	Jumping velocity of a dislocation during serrated yielding.
C_1	Solute concentration at the dislocation line.
C_o	Solute concentration of the alloy.
ℓ_d	Length between attractive trees of defect.
ρ_o	The density of randomly distributed dislocation network.
σ_y, σ_o	0.2% tensile yield stress of the alloy and solid solution.
a_o	A lattice parameter.
F_A, F_B	The atomic fraction of A and B atoms.
τ_{AP}	The applied shear stress.
$\bar{L}$	The mean planar particle spacing.

α, α_1, A, A_1, A_2, A_s, β, B_1, B_2, B_3, K', m, n, N
Constants arising in the analysis of serrated yielding process.

κ Boltzmann's constant; 1.381×10^{-16} erg/K°.

A_o The area occupied by a loop.

dN The number of attractive trees per unit volume

β_1, B, δ, $N_{hk\ell}$, $\bar{V}_{LI_2}$ Constants arising in the particle strengthening process.

γ_θ The dislocation loop radius.

Z_{AB} The number of first nearest neighbor atoms in crystal.

$\Delta\sigma_f$ The discontinuous increase in flow stress prior to the yield drop.

$\Delta\sigma_d$ The displacement of the level of the force-elongation curve accompanying each serration.

ε_s The strain between successive periodic locking serrations.

e Engineering strain.

v, β', $\bar{A}$ Constants arising in the analysis of coarsening process.

$f(\bar{r}, \bar{f}_v)$ A function of particle size and volume fraction of γ'.

a_p, a_m Lattice parameters of the precipitate particle and the matrix respectively.

ε_p Plastic strain.

ACKNOWLEDGMENTS

I wish to express my sincere thanks to my supervisor, Dr. M. C. Chaturvedi whose guidance and assistance made this work possible. In addition, I am indebted to Dr. D. J. Lloyd for making many helpful suggestions for the improvement of this thesis. I also acknowledge the University of Manitoba for financial support in the form of a scholarship.

Above all, I am grateful to my wife, Myong Hi for her faithful patience and encouragement during the course of this study.

CONTENTS

		Pages
	ABSTRACT	a
	SYMBOLS	d
	ACKNOWLEDGEMENT	i
I	INTRODUCTION	1
II	LITERATURES	4
1.0	Coarsening Process of precipitate particles	4
1.1	Diffusion controlled growth kinetics	5
1.2	Distribution of particle size	8
1.3	The effect of volume fraction of the particle coarsening process	9
1.4	Experimental observations of coarsening kinetics	10
2.0	Strengthening mechanisms in alloys containing the precipitate particles	14
2.1	Particle shearing models	17
2.2	Particle by-passing model	21
2.3	Experimental evaluations of strengthening mechanism in precipitation hardened alloys	24
3.0	Serrated yielding behavior	28
3.1	Dynamic strain ageing model	28
3.2	Static strain ageing model	30
3.3	The relation between vacancy concentration and plastic strain	32
3.4	The relation between the critical strain, ε_c, obstacles spacing, L and the concentration of solute atoms, C_o	35
III	EXPERIMENTAL PROCEDURES	39
1.	Preparations of materials	39
1.1	Electro-polishing and etching	40

CONTENTS

		Pages
1.2	Carbon extraction replication	40
1.3	Electrolytic extraction of particles	40
1.4	Thin foil technique	41
2.	The measurement of particle size	42
3.	Deformation method	43
IV	EXPERIMENTAL RESULTS	46
1.	Precipitation behavior of alloys	46
2.	The coarsening behavior	53
2.1	Growth kinetics of γ'	53
2.2	The effect of volume fraction on the growth kinetics of γ'	54
2.3	Activation energy for the growth of the γ' particles	61
2.4	Distribution of particle size of γ'	63
3.	Deformation behavior	64
3.1	Yielding behavior	64
3.1.1	Dislocation structures	70
3.1.2	Determination of Anti phase boundary energy	72
3.2	Serrated yielding behavior	80
3.2.1	The characteristics of serrated yielding	81
3.2.2	Critical strain-temperature relationship	86
3.2.3	Critical strain-strain rate relationship	94
3.2.4	Determination of activation energy, Q_m	97
3.2.5	Development of m and β	97
3.2.6	The value of L	100
3.2.7	Effect of C_o and L on ε_c, m+β, and Q_m value	103
3.2.8	Electron microscopy	116

CONTENTS

		Pages
V	DISCUSSION	120
1.	The growth kinetics of γ' phase	120
1.2	Effect of volume fraction of γ' on coarsening process	123
2.	Strengthening mechanism	124
2.1	Strengthening mechanism during the early stage of ageing	125
2.1.1	Coherency strengthening	125
2.1.2	Order strengthening	127
2.1.3	Order strengthening vs coherency strengthening	129
2.2	Strengthening mechanism in overaged alloys	132
3.	Serrated yielding	134
3.1	Critical strain to serrations, ε_c	136
3.2.1	Vacancy production and mobile dislocation density-($m+\beta$)	136
3.3	The influence of solute content, C_o	137
3.4.1	The influence of particle spacing, $\bar{L}$	138
3.5	Activation energy	140
3.6	Comparison with previous experiments	143
VI	CONCLUSIONS	145
VII	REFERENCES	148

I. INTRODUCTION

The empirical development of an alloy for the improvement of its mechanical properties has led to introducing a variety of alloying element into the more complex alloying system. During the past several years many nickel and cobalt based superalloys have been developed. These alloys have been extensively used in exacting thermal conditions because of their good mechanical and corrosion properties. Cobalt based superalloys have a flatter stress-rupture/time temperature parameters, can provide a better hot corrosion resistance, and also they can be used at temperature a few hundred degrees higher than Nickel base alloys[1]. Most of the strength of these high temperature superalloys is derived by the precipitation of γ' phase. The γ' precipitate is of Ni_3X type with an ordered F.C.C. structure (LI_2), and precipitates coherently in the F.C.C. matrix of nickel base alloys. The magnitude of the strength of these alloys is dependent mainly on the volume fraction and size of γ' precipitate and also on their growth kinetics.

The coarsening process of spherical particles in a fluid matrix has been explained in terms of a diffusion controlled process[2,3]. A similar explanation has been successfully applied to the growth of γ' particles in the solid state in several binary Ni - base alloys[4-7]. In addition, this type of precipitate has also been shown to possess the diffusion controlled coarsening characteristics in a low volume fraction alloy Nimonic 80A[8], as well as in a high volume fraction alloy, Udimet 700[9].

Following the coarsening kinetics of γ' phase, several strengthening mechanisms by γ' particles in terms of dislocation interaction with particles have been widely investigated in Nickel-base high temperature alloys[10-12]. When the γ' particles are small the moving dislocation tends to shear the particle and when the particle size is large it by-passes them by the Orowan mechanism.

During the particle shearing, the strength of the alloy seems to be governed mainly, by two factors, viz. (1) chemical or order hardening and (2) coherency or misfit hardening. The chemical hardening originates from the anti-phase boundary which is created within the ordered particles during the shearing process[12]. The coherency hardening is attributed to the interaction of glide dislocations with the elastic coherency stresses around coherent γ' precipitates. A great deal of doubt exists regarding the relative contribution of these two factors to the strength of alloys. Mihalison and Decker[13], and Fine[14] emphasize the coherency strains while Raynor and Silcock[15] and Phillips[16] consider A.P.B. energy to be the main strengthening factor. On the other hand, Singhal and Martin[17] found the two factors to be additive. However, at large misfit, coherency strain will be more significant than at low misfit.

During the course of the deformation studies serrated yielding has been noted in superalloys[18]. An extensive literature has been developed regarding the serrated yielding in F.C.C. and B.C.C. alloys[19-21], but there has been no detailed investigation of the phenomenon in alloys precipitation hardened by γ' phase. In the case of Udimet 520[19],

Doi and Shimanuki attributed the effect to solute atom-dislocation interaction, similar to the mechanism suggested for the majority of F.C.C. alloys. However, serrated yielding in a series of metastable austenitic alloys has been attributed to carbide precipitation. But, the influence of large amount of second phase particle on serrated flow has not been investigated in any detail. In Al alloys Phillips[22] and Matsuura et al[23] have shown that ageing increases the critical strain to serrations and may also modify the nature of serrations observed. Experiments on Alpha-beta brass[24] have also shown that the critical strain to serrations increases with increasing volume fractions of second phase. However, the mechanism by which precipitation influences serrated yielding is not understood at present.

Recently in a Co - Ni - Cr - Ti alloy[25], the main strengthening phase was identified as the γ' ordered, Ni_3Ti, which precipitates coherently in a Co - Ni - Cr F.C.C. matrix and on overageing γ' transforms to a hexagonal η- type, Ni_3Ti phase. The lattice misfit between γ and γ' was found to be 1.3%, which is one of the higher values in comparison with those of other high temperature alloys[25].

This alloy was chosen as the basic composition to investigate the coarsening behavior of γ' precipitate as well as its influence on the deformation behavior in a series of Co - Ni - Cr - Ti alloys.

II LITERATURE REVIEW

1. Coarsening process of precipitate particles.

The mechanical properties of precipitation strengthened alloys have been understood in terms of the morphological changes through the thermal interaction between the two phases. These changes usually involve the shapes and sizes of the second phase particles and their distribution. The shape changes may be related to diffusion along the interface of the particles while the change in size is controlled by the volume diffusion of the particles and/or by the volume diffusion within the matrix surrounding the particles. The change in size distribution may also be controlled by the mechanism of transport across the interface of the particles, and/or by the diffusion in the matrix. Early in 1900, Ostwald[26] first reported a systematic study of the increased solubility of small particles due to their reduction in total particle surface (Ostwald ripening). Later, Lifshitz and Slyozov[2] and Wagner[3] developed the basic theory of particle coarsening (LSW theory). Several reviews on this problem have recently appeared in the literature, e.g. by Greenwood, [27] by Che-Yu Li and Oriani[28] and by Ardell[29].

The basic theory of LSW is concerned primarily with the fact that if there is enough atomic mobility in a solid matrix, a dispersion of particles will coarsen by the transfer of matter from small to large particles in order to reduce the free energy associated with the particle/matrix interface area. In other words, at any given moment, particles smaller than a critical size r* will dissolve, surrounding themselves with an excess amount of solute atom which will diffuse to particles larger than r*. Thus, if the diffusion of atoms between

the particles is the slowest step, then the coarsening will be diffusion controlled, whereas if the deposition or dissolution of atoms at the particle interfaces is the slowest step then the growth kinetics will be the reaction controlling process. Based on these definitions the concentration profile between particles can be constructed as shown in Figure (1), and several growth rates of the particle can be formulated. (The case of interface controlled transfer also developed by Wagner[3] will not be considered here.)

1.1 Diffusion controlled growth kinetics.

The coarsening process where the rate determining step is the diffusion through the matrix has been analysed by Wagner[3].

He began with the old classic Gibbs-Thomson equation

$$C_r = C_e \exp (2 \gamma_s \Omega / r RT) \quad .... \quad (1)$$

relating C_r, the equilibrium solubility of a one component particle of radius r, to C_e, the equilibrium solubility of a particle of infinite radius in the given external fluid phase. γ_s is the specific interfacial free energy between the external phase and the particle of molar volume Ω, R is the gas constant and T the absolute temperature.

Using Zener's expression[30] for the concentration gradient at the interface between the particle and solution, he obtained the rate of change in particle radius,

$$\frac{dr}{dt} = D\Omega \frac{C - C_r}{r} = \frac{\gamma_s C_e D \Omega}{RTr} \left(\frac{1}{r^*} - \frac{1}{r}\right) \quad .... \quad (2)$$

Figure (1) Schematic concentration profiles for growing and shrinking particles.

(a) pure surface control,

(b) fast diffusion or large particle spacings,

(c) slow diffusion or small spacings.

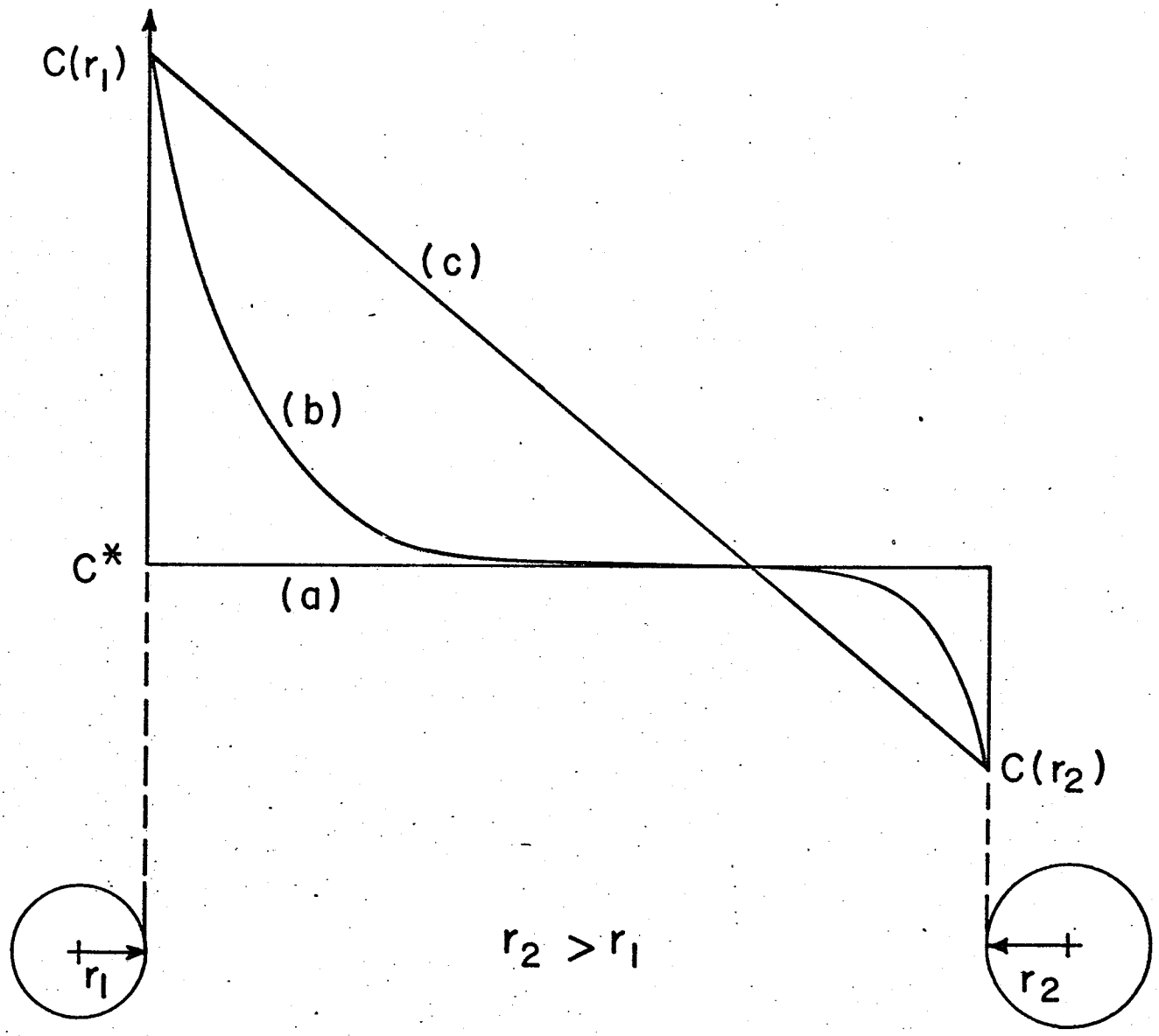

FIG. (1)

where D is the diffusivity in the matrix phase and r* is the critical radius given by

$$\Sigma\ r_i/\Sigma r_i^{\,2} = \frac{1}{r^*}$$

Provided the number of particle/unit volume is not too large the equation (2) may be applied to any one particle in an assembly of particles distributed at random over a range of size. It, however, should be noted that C denotes the mean concentration at the periphery of a sphere and also that the particle is drawn with a diameter equal to the mean separation between particles. Thus, the particle characterized by $C_r < C$, ie. larger than average particles in their immediate neighbourhood, will grow, and the particle characterized by $C_r > C$ ie. smaller than average will lose substance.

Wagner also solved the complex statistical problem for the variation of the mean radius $\bar{r}$ with time in an assembly of particles by introducing the size distribution function f(r,t). This function is such that f(r,t) dr is the number of particles at time t having radii between r and r + dr. (Details of solution are in Ref. (2) and (3).

The final form of LSW equation for the diffusion controlled process is thus given by

$$\bar{r}(t)^3 - \bar{r}(0)^3 = \left(\frac{8r_s DC_e\Omega^2}{9RT}\right)t = Kt \qquad \ldots\ (3)$$

where $\bar{r}(0)$ is the particle radius at the onset of coarsening.

This equation is valid only after the time required to deplete the concentration of matrix down to the C_e, and when the transfer of matter between particles is controlled by diffusion in the matrix.

1.2 Distribution of particle size.

Wagner[3] further showed that the distribution function of particle size f(r,t) is proportional to r^2, by

$$f(r,t) = g(t)\ \rho^2\ h(\rho) \qquad \ldots . \qquad (4)$$

where $g(t) = 1/(1 + t/\tau')^{4/3}$, $\tau' = \dfrac{9(\bar{r}(o))^3 RT}{8\gamma_s D C_e\ \Omega^2}$

$= (\bar{r}_{(o)})^3/K$, $\rho = r/r^*(t)$, and he also found $h(\rho)$ as

$$h(\rho) = \left(\frac{3}{3+\rho}\right)^{7/3} \left(\frac{3/2}{3/2-\rho}\right)^{11/3} \exp\left(\frac{-\rho}{3/2-\rho}\right) \quad \text{when } \rho < 3/2$$

$$h(\rho) = 0 \qquad \text{when } \rho > 3/2$$

The function $\rho^2 h(\rho)$ has the following characteristic features;

(a) a sharp cut-off at $\rho = 3/2$

(b) maximum at $\rho = 1.135$

(c) $\int_o^\infty \rho^2 h(\rho) d\rho = 9/4$ .... (5)

It has also been shown that, the distribution function f(r,t) is so defined that $\int_o^\infty f(r,t)\ dr = Z$, where Z is the number of particle/unit volume.

For the empirical purposes it is convenient to normalize f(r,t) by defining a new function g'(r,t) such that $\int_o^\infty g'(r,t)\ dr = 1$.

Upon substitution of equation (4) into the defining expression for Z, and making use of equation (5)

$$g'(r,t) = f(r,t)/Z$$

which then becomes

$$g'(r,t) = \frac{\rho^2 h(\rho)}{(9/4)\bar{r}}$$

Thus, for "steady-state" distribution the experimental histogram $g'(r,t)$ need only be multiplied by $(9/4)\bar{r}$ for comparison with the theoretical time-invariant function $\rho^2 h(\rho)$.

1.3 The effect of volume fraction on the particle coarsening process.

The theory of diffusion controlled particle coarsening developed by LSW is applicable only when the volume fraction, f_V, of the dispersed phase is very low. Just how small f_V must be is not precisely defined in the LSW theory. However it is assumed that it is small enough so that the mean distance between particle centers is larger than the particle dimension.

Sarian and Weart[31] suggested that the general growth law of LSW theory was still valid with a finite fraction f_V of precipitates. The only difference was that the rate constant in equation (3) had to be multiplied by a f_V dependent enhancement factor given by $4/3[(1 - f_V)/f_V]^{-1}$. Recently Ardell[32] modified the LSW theory in that the coarsening rate should increase with increasing volume fraction of precipitate, whereas the basic $(1/t)^3$ kinetics are unaffected. According to this modification, even at very small volume fraction ($f_V < 0.01$) the effect of f_V on the

coarsening rate is significant as shown in Fig. (2). It was clearly indicated that Ardell's approximation for critical radius, r*, would exaggerate the effect of particle interaction and therefore could be considered as an upper bound. Furthermore Ardell predicted that the theoretical distribution function of particle size should also be affected by f_V. Figure (3) shows the effect of volume fraction on the diffusion controlled growth. It is seen that $h(\rho)$ broadens rapidly with increasing f_V, and approaches the particle size distribution for interface coarsening in the limit $f_V = 1$.

1.4 Experimental observations of coarsening kinetics.

The first experimental evidence supporting the theory of diffusion controlled particle growth in a solid was obtained by Livingston[33]. Working on Co precipitate in Cu - Co alloys, he found a cubic growth kinetics by magnetic technique. A later study by Servi and Turnbull[34] verified that the growth of precipitate in this system is diffusion controlled. Both studies, however, deal with early stages of precipitate growth, and it is not certain that Livingston's result pertain to stationary Ostwald ripening.

Speich and Oriani[35] found that the growth of Cu precipitate is Cu - Fe matrix follows a cubic rate law, even though the precipitates are rod shaped. However, a number of complicating features were left in the application of LSW theory in this system since the precipitates are semi coherent in the matrix. A considerable amount of attention has recently been given to the influence of coherency strain on the particle growth kinetics[36-38]. It has been

Figure (2) Effect of Volume fraction of particles on rate constant, $K^{(32)}$.

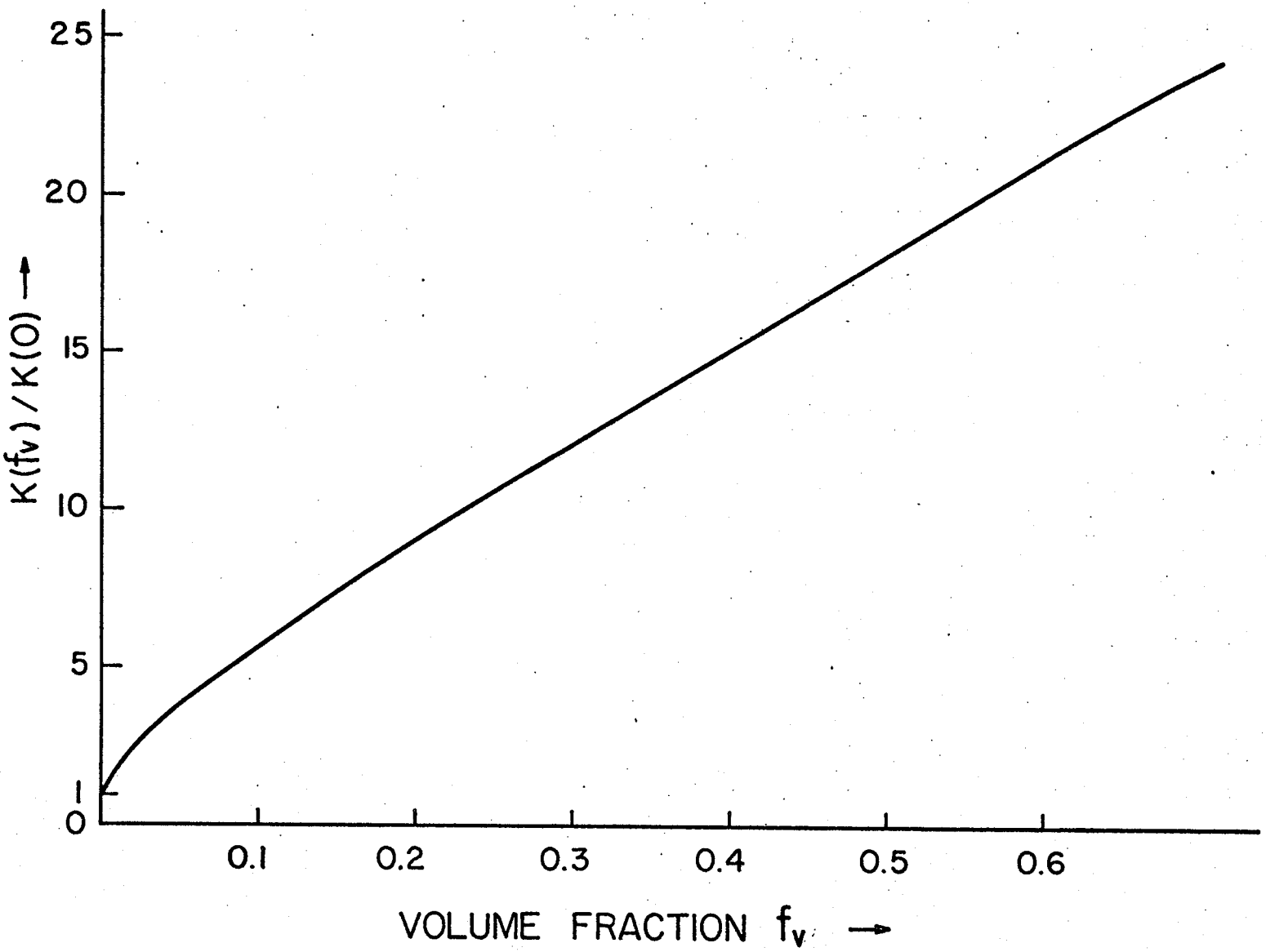

FIG. (2)

Figure (3) Stationary size distributions[2,3] and the effect of volume fraction in diffusion controlled growth[32].

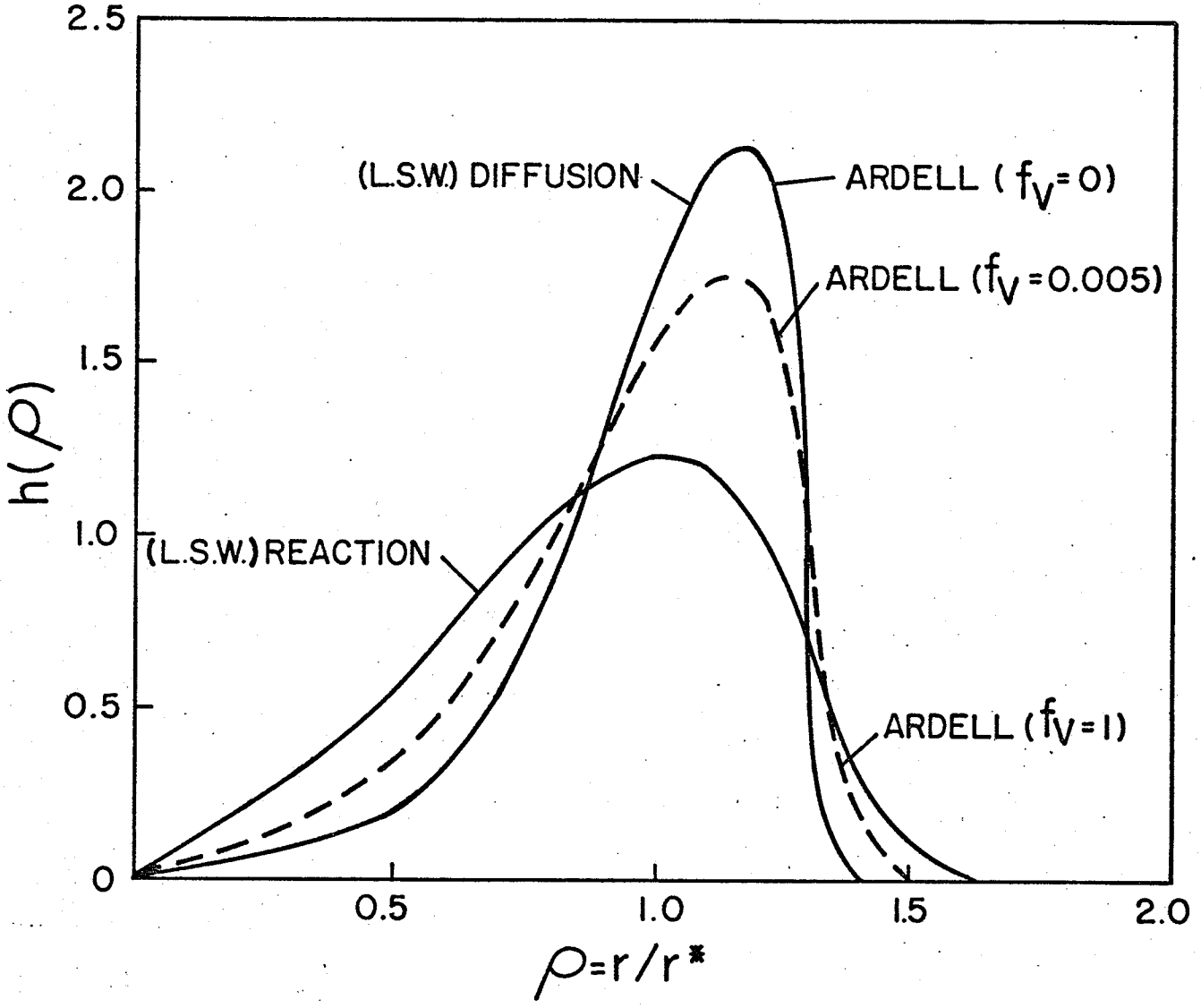
2.5
2.0
1.5
1.0
0.5
0
h(ρ)
(L.S.W.) DIFFUSION
ARDELL (f_V = 0)
ARDELL (f_V = 0.005)
(L.S.W.) REACTION
ARDELL (f_V = 1)
0.5
1.0
1.5
2.0
ρ = r / r*

FIG. (3)

argued that a coherent precipitate, because of its associated strain energy, must have a higher solubility than a non-coherent precipitate of the same phase. Although some alteration in the growth parameter has been made, serious modification to the general form of the growth analysis is not expected to be required[38].

Most of the coarsening studies on metal - intermetallic systems have been concerned with γ' phase [Ni_3(Al, Ti)] particles in nickel based alloys. This subject has been well reviewed by Ardell[29] and Hornbogen and Roth[39]. Generally the γ' particles are coherent with the matrix, but in Ni - Cr - Al alloy, by adjusting the matrix composition the misfit can be made zero. It is also found that the particle/matrix interface energy is very low since only second nearest neighbor interactions are involved. With increasing misfit the particle shape can change from spherical to cubic and finally plate or rod-like. Frequently a large volume fraction of γ' precipitate is developed in these alloys. The precipitate particles, then, align themselves along <100> directions owing to the interaction of coherency stresses. Eshelby[40] has discussed these interactions in detail and a mechanism for alignment by preferential growth of favorably situated particles has been proposed[4]. However, irrespective of particle shape and misfit, growth of the γ' precipitate obeys a diffusion controlled coarsening model where the average particle radius increases linearly with time to the one-third power, $t^{1/3}$. i.e. $\bar{r} \propto t^{1/3}$.

In the case of superalloy containing γ' phase Mitchell[8] has shown that the coarsening of γ' in the relatively simple, low volume fraction superalloy Nimonic 80A is also diffusion - controlled.